The author thanks V. K. Andreev for his interest in this work.

LITERATURE CITED

1. J. R. A. Pearson, "Convection cells induced by surface tension," J. Fluid Mech., 4, No. 5 (1958).
2. L. E. Scriven and C. V. Sternling, "Cellular convection driven by surface tension gradients: effect of mean surface tension and surface viscosity," J. Fluid Mech., 19, No. 3 (1964).
3. M. Ya. Antimirov and V. R. Liepinya, "Onset of thermocapillary convection in a cylindrical layer of fluid in conditions of weightlessness," Izv. LatvSSR Ser. Fiz. Tekh. Nauk, No. 3 (1978).
4. V. K. Andreev, A. A. Rodionov, and E. A. Ryabitskii, "Onset of thermocapillary convection in a fluid cylinder, cylindrical and plane layers under the influence of internal heat sources," Zh. Prikl. Mekh. Tekh. Fiz., No. 2 (1989).
5. A. Vidal and A. Acrivos, "Nature of the neutral state in surface tension driven convection," Phys. Fluids, 9, No. 3 (1966).
6. V. A. Urpin and D. G. Yakovlev, "Excitation of capillary waves in nonuniformly heated fluid films," Zh. Tekh. Fiz., 59, No. 2 (1989).
7. H. Lamb, Hydrodynamics, Dover, New York (1932).
8. S. Chandrasekhar, Hydrodynamic and Hydromagnetic Stability, Oxford University Press (1961).
9. V. K. Andreev and E. A. Ryabitskii, Small Perturbations of Thermocapillary Motion in the case of a Cylinder [in Russian], Moscow, (1984), Deposit in VINITI, No. 7788-84 (27.11.84).

CALCULATION OF THE FLOW FIELD PAST SPHERICALLY BLUNTED CONES NEAR THE PLANE OF SYMMETRY FOR VARIOUS SHOCK LAYER FLOW REGIMES WITH INSUFFLATION OF GAS FROM THE SURFACE

A. V. Bureev and V. I. Zinchenko

UDC 533.6.011.536.24

We investigated flow past a cone, which has been blunted in a spherical fashion, over a wide range of Reynolds numbers. Various flow regimes were realized in the shock layer. The study was done within the framework of a completely viscous shock layer model, near the plane of symmetry of the flow. In the shock layer for this flow, the problem of self-consistent calculation for the plane of symmetry was treated in [1, 2] by means of a Fourier series expansion of the pressure in terms of the circumferential coordinate. In [3], a prescribed pressure gradient in the circumferential coordinate taken from tables of inviscid flow was used to model a thin viscous shock layer. Here, we apply the truncated series procedure [4], and analyze the effect of the angle of attack α_A and taper angle β on the heat exchange characteristics. The case where α_A is significantly larger than β is included in our analysis. We also analyze the effect of discharge quantity and the distribution law of gas insufflating through a porous, spherical shell on the heat exchange characteristics.

1. Let us write out the system of equations for a viscous shock layer in the neighborhood of the flow plane of symmetry in the natural coordinate system (s, ψ, n), attached to the body axis of symmetry. Using an expansion of the coefficients and unknown functions of the form

$$f = f_0 + f_2\psi^2 + \ldots \ (f = u,\ v,\ H,\ \rho,\ \mu,\ p,\ h,\ n_s),$$
$$\omega = \omega_1\psi + \ldots$$

Tomsk. Translated from Prikladnaya Mekhanika i Tekhnicheskaya Fizika, No. 6, pp. 72-78, November-December, 1991. Original article submitted July 26, 1990.

0021-8944/91/3206-0887$12.50

to an accuracy of $O(\psi^2)$, we obtain for averaged characteristics, the following system of equations (introducing dimensionless variables) [5]:

$$\frac{\partial}{\partial s}(\rho_0 u_0 r) + \rho_0 h_1 \omega_1 + \frac{\partial}{\partial n}(\rho_0 v_0 r h_1) = 0, \tag{1.1}$$

$$\frac{\rho_0 u_0}{h_1}\frac{\partial u_0}{\partial s} + \rho_0 v_0 \frac{\partial u_0}{\partial n} + \frac{k}{h_1}\rho_0 u_0 v_0 = -\frac{1}{h_1}\frac{\partial p_0}{\partial s} + \tag{1.2}$$

$$+ \varepsilon^2 \frac{\partial}{\partial n}\left[\mu_\Sigma\left(\frac{\partial u_0}{\partial n} - \frac{k u_0}{h_1}\right)\right] + \varepsilon^2 \mu_\Sigma\left(\frac{2k}{h_1} + \frac{\cos\alpha}{r}\right)\left(\frac{\partial u_0}{\partial n} - \frac{k u_0}{h_1}\right);$$

$$\frac{\rho_0 u_0}{h_1}\frac{\partial \omega_1}{\partial s} + \rho_0 v_0 \frac{\partial \omega_1}{\partial n} + \frac{\rho_0 \omega_1^2}{r} + \frac{1}{h_1 r}\frac{\partial r}{\partial s}\rho_0 u_0 \omega_1 + \frac{\cos\alpha}{r}\rho_0 \omega_1 v_0 = \tag{1.3}$$

$$= -\frac{2p_2}{r} + \varepsilon^2 \frac{\partial}{\partial n}\left[\mu_\Sigma\left(\frac{\partial \omega_1}{\partial n} - \frac{\omega_1}{r}\cos\alpha\right)\right] + \varepsilon^2 \mu_\Sigma\left(\frac{\partial \omega_1}{\partial n} - \frac{\omega_1}{r}\cos\alpha\right)\left(2\frac{\cos\alpha}{r} + \frac{k}{h_1}\right);$$

$$\frac{\rho_0 u_0}{h_1}\frac{\partial v_0}{\partial s} + \rho_0 v_0 \frac{\partial v_0}{\partial n} - \frac{k\rho_0 u_0^2}{h_1} = -\frac{\partial p_0}{\partial n}; \tag{1.4}$$

$$\frac{\cos\alpha}{r}\rho_0 \omega_1^2 = -\frac{\partial p_2}{\partial n}; \tag{1.5}$$

$$\frac{\rho_0 u_0}{h_1}\frac{\partial H_0}{\partial s} + \rho_0 v_0 \frac{\partial H_0}{\partial n} - v_0\left(\frac{\partial p_0}{\partial n} - \frac{k}{h_1}\rho_0 u_0^2\right) = \tag{1.6}$$

$$= \varepsilon^2 \frac{\partial}{\partial n}\left\{\frac{\mu_\Sigma}{\mathrm{Pr}_\Sigma}\left[\frac{\partial H_0}{\partial n} + (\mathrm{Pr}_\Sigma - 1)\frac{\partial}{\partial n}\left(\frac{u_0^2}{2}\right)\right] - \mu_\Sigma \frac{u_0^2 k}{h_1}\right\} +$$

$$+ \varepsilon^2\left(\frac{k}{h_1} + \frac{\cos\alpha}{r}\right)\left\{\frac{\mu_\Sigma}{\mathrm{Pr}_\Sigma}\left[\frac{\partial H_0}{\partial n} + (\mathrm{Pr}_\Sigma - 1)\frac{\partial}{\partial n}\left(\frac{u_0^2}{2}\right)\right] - \mu_\Sigma \frac{u_0^2 k}{h_1}\right\};$$

$$p_0 = \rho_0 h_0 \frac{\gamma - 1}{\gamma}. \tag{1.7}$$

We write the Rankine–Hugoniot relations on the windward side in the neighborhood of the flow plane of symmetry at the shock wave $n = n_S$. For the Reynolds number range of interest, these are:

$$u_{s0} = \cos(\alpha_A + \sigma)\cos\beta_s + \frac{1}{\rho_{s0}}\sin\beta_s \sin(\alpha_A + \sigma), \tag{1.8}$$

$$\omega_{s1} = \sin\alpha_A - 2\cos\beta_s\left(\frac{1}{\rho_{s0}} - 1\right)\sin(\alpha_A + \sigma)\frac{n_{s2}}{r_s},$$

$$v_{s0} = \cos(\alpha_A + \sigma)\sin\beta_s - \frac{1}{\rho_{s0}}\cos\beta_s \sin(\alpha_A + \sigma),$$

$$p_{s0} = \frac{(1-\gamma)}{\gamma(1+\gamma)M_\infty^2} + \frac{2}{(\gamma+1)}\sin^2(\sigma + \alpha_A),$$

$$p_{s2} = -\frac{2}{(\gamma+1)}\sin\alpha_A \sin(\sigma + \alpha_A)\cos\sigma,$$

$$\frac{1}{\rho_{s0}} = \frac{\gamma-1}{\gamma+1} + \frac{2}{M_\infty^2(\gamma+1)\sin^2(\sigma+\alpha_A)}, \quad H_{s0} = H_\infty = \frac{1}{2} + \frac{1}{M_\infty^2(\gamma-1)}.$$

When reading off the coordinate ψ from the plane of symmetry on the leeward side in (1.8), one must change α_A to $-\alpha_A$.

A manifestation of the elliptical character of the problem, due to the boundary conditions, is the presence in ω_{S1} of the second term, which characterizes the curvature of the shock wave surface with respect to the circumferential coordinate. When solving the problem, we analyzed the influence of n_{S2} on the characteristics of the flow in the neighborhood of the symmetry plane.

During insufflation there is, at the body ($n = 0$), the same state as in the incoming flux,

$$u_0 = \omega_1 = 0, \ (\rho_0 v_0) = (\rho_0 v_0)_w(s), \ h_0 = h_{0w}. \tag{1.9}$$

The angle of incidence of the shock wave with respect to the plane of symmetry σ is related to the outflux n_{S0} by the relation $dn_{S0}/ds = h_{1S}\tan\beta_S$, where $\beta_S = \sigma - \alpha$.

In (1.1)-(1.9) and below, u, ω, v are components of the vector velocity in the longitudinal and circumferential directions, and along the normal to the body which tends to v_∞; p, ρ are the gas pressure and density, tending to $-\rho_\infty v^2_\infty$ and ρ_∞, respectively; $H = h + u^2/2$ is the enthalpy tending to $\frac{1}{2}v^2_\infty$; T is the temperature, tending to characteristic value $T_* = v^2_\infty/c_p$; μ is the coefficient of viscosity, which tends to its characteristic value $\mu_*(T_*)$; $h_1 = 1 + kn$, $r = r_w + n\cos\alpha$ are the Lamé coefficients; α is the angle of inclination formed with respect to the body axis of symmetry; $\varepsilon^2 = \mu_*/(\rho_\infty v_\infty R_N)$ is a dimensionless parameter (the inverse Reynolds number); $\mu_\Sigma = \mu_0 + \Gamma\mu_T$; $Pr_\Sigma = \mu_\Sigma Pr Pr_T/(\mu Pr_T + \Gamma\mu_T Pr)$.

The coefficient of molecular viscosity is determined by the Sutherland formula

$$\mu = \left(\frac{1+C}{T+C}\right)T^{3/2}, \quad C = \frac{110{,}4}{(\gamma-1)M^2_\infty T_{\infty d}} \tag{1.10}$$

($T_{\infty d}$ is the dimensional temperature).

For the coefficient of turbulent viscosity μ_T, we used a two-layer model [6], which in the dimensionless variables adopted here can be written in the near-wall region

$$\mu_T = \frac{0{,}16\rho_0 n^2}{\varepsilon^2}\left[1 - \exp\left(-\frac{n}{A}\right)\right]^2\frac{\partial u_0}{\partial n}, \tag{1.11}$$

$$A = \varepsilon^2\frac{26\mu_0}{\rho_0 v_*}\left[\frac{\bar{P}}{\bar{v}_w}(1 - \exp(11{,}8\bar{v}_w)) + \exp(11{,}8\bar{v}_w)\right]^{-1/2},$$

$$v_w = \frac{v_w}{v_*}, \quad v_* = \varepsilon\sqrt{\frac{\tau_w}{\rho_0}}, \quad \bar{P} = -\frac{\varepsilon^2\mu_0}{\rho_0\rho_{w0}v^3_*}\frac{\partial p_{e0}}{\partial s}, \quad \tau_w = \mu_{w0}\frac{\partial u_0}{\partial n}\Big|_w,$$

and in the outer region

$$\mu_T = \frac{0{,}0168}{\varepsilon^2}\rho_0\left[1 + 5{,}5\left(\frac{n}{n_e}\right)^6\right]^{-1}\int_0^{n_e}(u_{e0} - u_0)\,dn. \tag{1.12}$$

The subscripts ∞, s, w, e are used to designate flow characteristics in the incoming flux, behind the shock wave, at the wall and quantities on the outer boundary layer of the shock layer, respectively. The subscript T denotes the characteristic of turbulent transport.

Calculation of the transition region of the flow was done with the help of formulas from [7]. For flow past a spherically blunted body, the coefficient of intermittance Γ, in a coordinate system attached to the stagnation point, has the form

$$\Gamma = 1 - \exp\left[-\frac{\Phi\sin s'}{\left.\frac{du_e}{ds'}\right|_{s'=0}}\ln\left|\frac{\operatorname{tg}\frac{s'}{2}}{\operatorname{tg}\frac{s'_\ell}{2}}\right|\ln\left(\frac{s'}{s'_\ell}\right)\right],$$

$$\Phi = \frac{3u^3_e}{\varepsilon^4\left(B\frac{\mu_e}{\rho_e}\right)^2}\mathrm{Re}_\ell^{-1{,}34}, \quad B = 60 + 4{,}68\,M_\ell^{1{,}92}.$$

Here $\mathrm{Re}_\ell = \frac{1}{\varepsilon^2}\frac{\rho_e u_e s'_\ell}{\mu_e}$, $M_\ell = \left(\frac{u_e}{a_e}\right)_{s'=s'_\ell}$ are the Reynolds and Mach numbers on the outer boundary at the point of stability loss for the laminar boundary layer. The coordinate of the point of stability loss s'_ℓ, which corresponds to the start of the transition flow region, is established from experiment, or calculated according to the critical value of the Reynolds number

$$\mathrm{Re}^{**} = \frac{1}{\varepsilon^2}\frac{\rho_e u_e \delta^{**}}{\mu_e} = 200, \quad \delta^{**} = \int_0^{n_e}\frac{\rho u}{\rho_e u_e}\left(1 - \frac{u}{u_e}\right)dn.$$

In the region of laminar flow, Γ = 0, while in the region of developed turbulence, Γ = 1.

2. The boundary-value problem described above is elliptical in character, and those methods based on global iterations along the form of the shock wave [5, 8] are effective methods for its solution. In calculating the system of equations (1.1)-(1.7), we used the independent variables transformations [8]

$$\xi = s, \quad \eta = \frac{1}{\Delta}\int_0^n \rho_0\left(\frac{r}{r_w}\right)dn, \quad \Delta = \int_0^{n_s} \rho_0\left(\frac{r}{r_w}\right)dn.$$

Within the framework of each global iteration, computation of the spherically blunted body is carried out in a coordinate system attached to the stagnation point of the flow. In this coordinate system, the flow is axisymmetric by procedure [9]. The subsequently obtained profiles u', v' were recalculated near the transition to the initial coordinate system (s, ψ, n) according to the formulas $v_0 = v'$, $u_0 = u'$, $\omega_1 = u' \sin\alpha_A/\sin(s - \alpha_A)$ and was solved as a continuation problem.

In obtaining difference schemes for the parabolic and hyperbolic equations, the iteration-interpolation method [10] was applied. For the turbulent flow regimes, we devised composite difference schemes which took into account the character of the change in the coefficient of turbulent viscosity perpendicular to the shock layer. This made it possible to carry out calculations up to Re $\approx 10^8$-10^9 for various values of the insufflating gas discharge from the surface of the body. Numerical integration of systems of parabolic and hyperbolic equations in the subsonic and predominately supersonic regions of the flow was done with the help of vectorization, which, within the limits of the global iteration, increases the stability and improves convergence of the iteration process. The organization of the global iteration coincides with that of [9]. The solution required several global iterations.

3. Calculations of flow past a cone blunted in a spherical manner were carried out for values of the governing parameters corresponding to those for an experimental study of models in a wind tunnel [11]. Figures 1, 2 show the effect of the angle of attack on the aerodynamic characteristics and heat fluxes towards the surface on the windward side for flow past a cone with half-angle $\beta = 5°$, and radius of spherical truncation $R_N = 0.0508$ m for experimental conditions [11]: $M_\infty = 5$, stagnation point temperature $T_{e0} = 525$ K, $T_w = 288$ K, stagnation point pressure $p_{e0} = 0.625\cdot10^5$, $3.125\cdot10^5$ N/m^2 for the laminar and turbulent flow regimes. For this case, the governing parameters for the original boundary-value problem are: $\gamma = 1.4$, $\varepsilon^2 = 1.13\cdot10^{-5}$, $2.14\cdot10^{-6}$ for the laminar and turbulent regimes, and $h_w = 0.33$.

In the absence of gas insufflation, Fig. 1 shows the pressure distribution at the surface p_w (curves 1 and 2), and the outflux n_{s0} (curves 1', 2') for angles of attack $\alpha_A = 0$ (curves 1, 1') and 12° (2, 2'). The coordinate system is attached to the stagnation point. The crosses indicate data from inviscid calculations, and the dashed line, data obtained from axisymmetric flow past a blunted cone of half-angle 17°. This data illustrates the possibility of applying the rule of local cones [12] to find gasdynamic quantities. For the indicated values of ε^2, the distribution of pressure and outflux is virtually unchanging. The effect of the angle of attack on the dimensionless heat flux $q_w = \left(\frac{\mu_0}{\mathrm{Pr}}\frac{\partial H_0}{\partial n}\right)_w \frac{\sqrt{\mathrm{Re}}}{\rho_{e0} v_s h_{e0}}$ (Re $= \rho_{e0} v_s R_N/\mu_{e0}$, $v_s = \sqrt{2h_{e0}}$, $e0$ corresponds to the stagnation point) for various flow regimes in the viscous shock layer is shown in Fig. 2, where curves 1 and 2 were obtained for $\alpha_A = 0$ and 1' and 2' correspond to $\alpha_A = 12°$ for the laminar and turbulent flow regimes, respectively. Here the symbols for $\alpha_A = 0$ denote experimental data [11]. The distribution $q_w(s')$ for $\alpha_A = 0$, $\beta = 17°$ coincides (within the accuracy of the plot) with the computational results for $\alpha_A = 12°$, $\beta = 5°$ in the shock layer for both flow regimes.

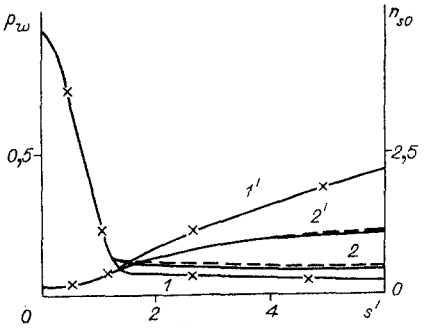

Fig. 1

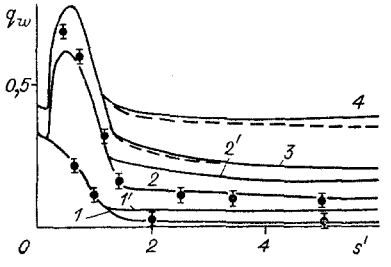

Fig. 2

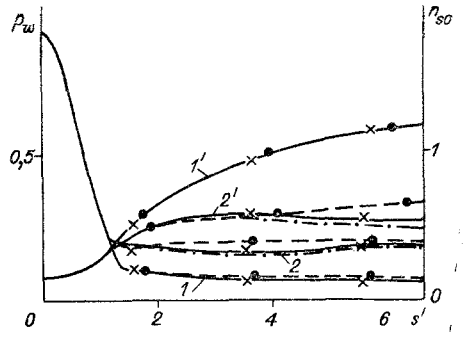

Fig. 3

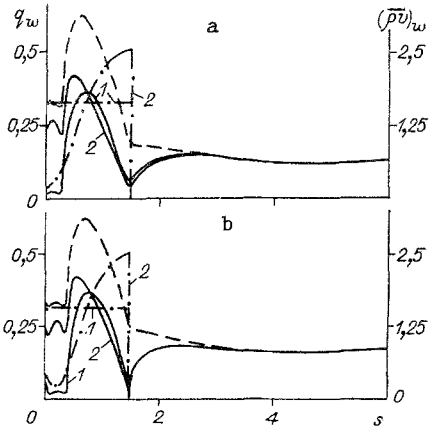

Fig. 4

The question arises of the degree of applicability of the problem setup used for growing angle of attack. For these same governing parameters, excluding M_∞, which was taken as equal to 6, Fig. 3 shows the distributions of p_w and n_{s0} for $\alpha_A = 10°$ (curves 1, 1') and 20° (curves 2, 2'). For $\alpha_A = 20°$, the solid curve is obtained by setting

$$\frac{n_{s2}}{r_s} = \frac{\sin\alpha_A}{2\left(1-\frac{1}{\rho_{s0}}\right)\sin(\sigma+\alpha_A)\cos\beta_s}\left[1-\frac{u^*_{s0}}{\sin(s_1-\alpha_A)}\right], \tag{3.1}$$

in the boundary condition (1.8), which corresponds to $\omega_{s1} = \sin\alpha_A \cdot u^*_{s0}/\sin(s_1 - \alpha_A)$. Here u^*_{s0} is the value of the longitudinal velocity component behind the shock wave, taken at the conjugate point s_1 of the spherical and conical parts of the body at the flow line. The dot-dash curves correspond to the case where the shape of the shock wave is similar to the body shape in the circumferential direction ($n_{s2}/r_s = 0$), and the dashed lines, to axisymmetric flow past a blunted cone with half-angles $\beta = 15$ and 25°, respectively. The crosses correspond to inviscid calculations for flow at angles of attack, the circles to calculations of axisymmetric inviscid flow past cones with half-angles $\beta = 15$ and 25° [13].

It is evident that when the angle of attack is significantly larger than the cone angle, neglecting the effect of the shock wave curvature in the circumferential direction has an effect on the governing aerodynamic characteristics of the body, and the calculation of axisymmetric flow of the equivalent cones shows significant error in the behavior of the pressure at the surface and outflux n_{s0}. Similar conclusions follow from the behavior of the heat fluxes along the generatrix $q_w(s')$, shown in Fig. 2 for the given conditions with $\alpha_A = 10$, 20° (curves 3 and 4). In turn, by means of a fairly simple method of sharpening the boundary conditions for ω_{s1}, we succeeded in significantly expanding the region of applicability of the initial setup with respect to the governing aerodynamic characteristics and the characteristics of heat and mass exchange on the weather side, in the flow plane of symmetry in those cases where α_A significantly exceeds β.

For insufflation of gas through a porous, truncated sphere, we examine the effect of the prescribed outflux law and the rate of gas insufflation on the heat flux towards the body, near the plane of symmetry on the windward side. For the above-mentioned governing parameters from [11], Fig. 4 shows the heat flux distribution q_w (solid curves 1 and 2) for the corresponding gas discharges (dot-dash curves 1 and 2) for (a) $\alpha_A = 6°$ and (b) $\alpha_A = 12°$. The dashed curves are for heat flux towards an impermeable surface, computed by using a coordinate system attached to the body axis of symmetry. For the prescribed dimensionless quantity $(\overline{\rho v})_w = (\rho v)_{w0}\sqrt{\mathrm{Re}}/\rho_{e0}v$ we examined the laws of change $(\overline{\rho v})_w(s) = \text{const} = 1.63$, 1.55 (curves 1 in Fig. 4a and 4b). We also used the discharge $(\rho v)_w(s)$ which follows from D'Arcy's law for a porous shell with a prescribed pressure in the shell cavity p_c

$$(\rho v)_w = \left[-A\mu + \sqrt{(A\mu)^2 + \frac{2B\varphi}{TL\frac{R}{M}}\left(p_c^2 - p_w^2\right)}\right]\frac{1}{2B}. \tag{3.2}$$

Here A, B are the coefficients in D'Arcy's law; ϕ is the porosity; and L is the shell thickness. In this case, the total mass of the coolant, insufflating on the windward side near

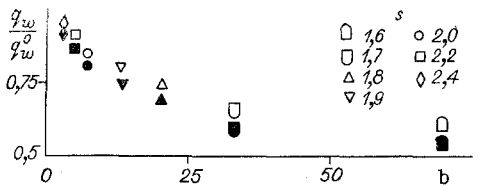

Fig. 5

the plane of symmetry $R_N^2\psi\int_{\alpha_A}^{s_1}(\rho v)_{w0}\sin s\,ds$ is taken as the same for both insufflation laws.

From the data given here, it is evident that, despite the fundamental differences in the heat flux distributions on the spherical part of the body, due to different discharge laws $(\overline{\rho v})_w(s)$, the length of the thermal screen zone is largely determined by the total mass of the insufflating gas-coolant. For the discharge laws considered here, it depends only weakly on the nature of the distribution $(\overline{\rho v})_w(s)$ on the spherical truncation. The pressure at the surface and outflux of the shock wave for the indicated insufflating gas discharge values are virtually unchanged.

As in [14], we carried out an analysis of the solution on the conical part of the body in the thermal screen zone for the turbulent flow regime. In the neighborhood of the plane of symmetry, on the windward side, we obtain for the insufflation parameter

$$b=\frac{2\int_{\alpha_A}^{s_1}(\rho v)_{w0}(s)\sin s\,ds\,(H_{e0}-h_w)}{q_w^0(s)(s-s_1)(r_{w1}+r_w)}.$$

This parameter characterizes the ratio of the mass of the insufflating gas to the product of the heat transfer coefficient in the cross section s (in the absence of insufflation) and a section of surface area (from the cut-off line of insufflation to the coordinate value).

Figure 5 shows the dependence of $q_w(s)/q^0{}_w(s)$ on b in the screen zone ($q^0{}_w$ is the heat flux in the given cross section in the absence of insufflation). The open and filled symbols correspond to constant discharge and to dependence (3.2) for various angles of attack. These results are in agreement with data for axisymmetric flow. The results make it possible to estimate the heat flux towards the cone surface in the thermal screen zone on the windward side, where maximum values of $q_w(s)$ are attained in the flow, for various angles of attack.

In conclusion, we express our deepest thanks to V. D. Gol'din for making computational results of inviscid flow past an object available to us.

LITERATURE CITED

1. A. Kumar and R. A. Graves, Jr., "Viscous hypersonic flow past blunted cones at small angles of attack," AIAA J., 15, No. 8 (1977).
2. A. Kumar, "Low Reynolds number flow past a blunt axisymmetric body at angles of attack," AIAA J., 15, No. 8 (1977).
3. R. R. Eaton and P. C. Kaestner, "Viscous shock-layer flow in the windward planes of cones at angles of attack," AIAA J., 11, No. 9 (1973).
4. K. N. Efimov and V. I. Zinchenko, "Numerical investigation the flow field of a hypersonic thin viscous shock layer in the neighborhood of a plane of symmetry," Model. Mekh., 1, No. 5 (1987).
5. R. T. Davis, "Numerical solution of the hypersonic viscous shock-layer equation," AIAA J., 8, No. 5 (1970).
6. T. Cebecu, "Behavior of turbulent flow near a porous wall with pressure gradient," AIAA J., 8, No. 12 (1970).
7. K. K. Chen and N. A. Tyson, "Extension of Emmons spot theory to flow on blunt bodies," AIAA J., 9, No. 5 (1971).
8. S. A. Vasil'evskii and G. A. Tirskii, "Some methods for numerical solution of the viscous shock layer equation," in: The Aerodynamics of Hypersonic Flow with Insufflation [in Russian], Mosk. Gos. Univ., Moscow (1979).

9. V. I. Zinchenko and S. I. Pyrkh, "Calculation of a nonequilibrium viscous shock layer and associated heat exchange," Izv. Akad. Nauk SSSR, Mekh. Zhid. Gaza, No. 2 (1984).
10. A. M. Grishin, V. N. Bertsum, and V. I. Zinchenko, The Iterative-Interpolation Method and Its Application [in Russian], Tomsk. Gos. Univ., Tomsk (1981).
11. R. H. Feldhuhm, "Heat transfer from a turbulent boundary layer on a porous hemisphere," AIAA Paper No. 119 (1976).
12. V. V. Lunev, Hypersonics [in Russian], Mashinostroenie, Moscow (1975).
13. A. N. Lyubinov and V. V. Rusanov, Gas Flow Past Blunt Bodies [in Russian], Part 1, Nauka, Moscow (1970).
14. V. N. Kharchenko, "Heat exchange in a hypersonic turbulent boundary layer with insufflation of cooling gases through a crack," Teplofiz. Vys. Temp., No. 1 (1972).

INFLUENCE OF RAREFACTION ON THE UNSTEADY IMPINGEMENT PROCESS OF AN UNDEREXPANDED SUPERSONIC JET ONTO A PERPENDICULAR OBSTACLE

A. V. Savin, E. I. Sokolov,
V. S. Favorskii, and I. V. Shatalov

UDC 533.6.011.8

The destruction of a steady flow in front of an obstacle placed perpendicular to the axis of an underexpanded supersonic jet is one of the most interesting physical phenomena in jet flows. The essential feature of this is that a smooth quasi-steady variation of distance h from the nozzle to the obstacle or of the pressure ratio of the jet $n = p_a/p_\infty$, leads to a sudden discontinuous breakdown of the steady flow: a wave structure in front of the obstacle begins to oscillate with frequency of order several kilohertz (with nozzle exit diameter d_a = 10 mm), while the pressure at the obstacle varies with the same frequency. In contrast to jet noise with constant inflow, which has a broadband spectrum, in an enclosed space the acoustic field has clearly defined discrete frequencies.

At present, there are several hypotheses [1-4] concerning the source of these oscillations, which attests to the absence of a generally accepted theory. Also unclear is the cause of the sharp transition to unsteady impingement. In this situation, to create a conclusive theory of this process, we expand the range of parameters over which this phenomenon has been studied; this is as instructive for numerical modeling as for experiments. In particular, until now there has been almost no study of the influence of viscosity on the process of unsteady jet impingement. Experimental results of this investigation are given below.

1. The experiments were conducted in a vacuum chamber of volume 10 m^3 with pressure $p_\infty = 10^2$-0.1 Pa. To measure the pressure, mechanical gauges, U-shaped manometers and thermocouple vacuum gauges were used. The full-scale pressures ranged from 10^5-10^2 Pa, which allowed variation of the Reynolds number Re_* from 5×10^2 to 5×10^3 for Mach numbers M_a from 1 to 3.35 and $n \leq 500$. The working gases were air and helium at temperature T_0 = 293 K. The receiver with the nozzle and the obstacle were installed on three-axis translation stages. The indices 0, *, a, and ∞ refer to stagnation, sonic, nozzle exit and ambient conditions, respectively.

To measure the pressure fluctuations at the obstacle, type IS-2156 piezoelectric transducers were used. The diameter of the active transducer surface was 1.5 mm, while the characteristic dimension of the jet under study was 25-30 mm. The resonant frequency of this transducer is greater than 100 kHz, which allows measurement of frequencies up to 50 kHz. The nonuniformity of the resonant frequencies of the transducers was checked by comparing frequency spectra of each transducer with that of a capacitive microphone (Bruel and Kjaer, model 4135). The discrepancy in the readings was lower than 3 dB in the range 0-40 kHz.

Leningrad. Translated from Prikladnaya Mekhanika i Tekhnicheskaya Fizika, No. 6, pp. 78-83, November-December, 1991. Original article submitted January 22, 1990; revision submitted June 12, 1990.

0021-8944/91/3206-0893$12.50